Structural Characterization of the Fibrillar Form of the Yeast *Saccharomyces cerevisiae* Prion Ure2p†

Luc Bousset,‡,§,|| Virginie Redeker,*,‡,§ Paulette Decottignies,⊥ Steven Dubois,§ Pierre Le Maréchal,⊥ and Ronald Melki*,§

Laboratoire d'Enzymologie et Biochimie Structurales, CNRS, 91198 Gif-sur-Yvette Cedex, France, and Institut de Biochimie, Université Paris-Sud, 91405 Orsay Cedex, France

Received January 23, 2004; Revised Manuscript Received March 1, 2004

ABSTRACT: The protein Ure2 from the yeast *Saccharomyces cerevisiae* has prion properties. It assembles in vitro into long, straight, insoluble fibrils that are similar to amyloids in that they bind Congo Red and show green-yellow birefringence and have an increased resistance to proteolysis. We recently showed that Ure2p fibrils assembled under physiologically relevant conditions are devoid of a cross-β-core. A model for fibril formation, where assembly is driven by non-native inter- and/or intramolecular interaction between Ure2p monomers following subtle conformational changes was proposed [Bousset et al. (2002) *EMBO J. 21*, 2903−2911]. An alternative model for the assembly of Ure2p into fibrils where assembly is driven by the stacking of 40−70 N-terminal amino acid residues of Ure2p into a central β-core running along the fibrils from which the C-terminal domains protrude was proposed [Baxa et al. (2003) *J. Biol. Chem. 278*, 43717−43727]. We show here that Ure2p fibril congophilia and the associated yellow-green birefringence in polarized light are not indicative that the fibrils are of amyloid nature. We map the structures of the fibrillar and soluble forms of Ure2p using limited proteolysis and identify the reaction products by microsequencing and mass spectrometry. Finally, we demonstrate that the C-terminal domain of Ure2p is tightly involved in the fibrillar scaffold using a sedimentation assay and a variant Ure2p where a highly specific cleavage site between the N- and C-terminal domains of the protein was engineered. Our results are inconsistent with the cross-β-core model and support the model for Ure2p assembly driven by subtle conformational changes and underline the influence of the natural context of the N-terminal domain on the assembly of Ure2p.

Prions are infectious proteins that perpetuate altered conformational states at the origin of transmissible spongiform encephalopathies in mammals (*1*) and nonmendelian inheritance in yeast and fungi (*2*, *3*). The molecular events that lead to the acquision and propagation of the transmissible altered conformation of this class of proteins are still unknown. It is thought that the main event is a major conformational change leading prion proteins to assemble into fibrils that propagate by recruitment of a conformational intermediate of soluble prion proteins (*4*). Although attracting, this view cannot account by itself for the transmissible properties of prion aggregates as other proteins involved in over 20 different deposition diseases (*5*) including Alzheimer's, Parkinson's, and Huntington's diseases (*6*, *7*) are unable to propagate the structural information at the origin of the prion concept.

The protein Ure2 propagates the [URE3] phenotype in the yeast *Saccharomyces cerevisiae* (*8*). Under its, functional, nonprion state, Ure2p is a soluble cytoplasmic protein involved in a signal transduction pathway that regulates the use of nitrogen sources (*9*). Ure2p loses its function in [URE3] cells. This event is thought to result from the assembly of the protein into high molecular mass oligomers which are peculiar in that they propagate the yet unknown transmissible structural information termed [URE3] (*2*, *10*).

Soluble Ure2p is a two-domain protein (*11*, *12*). Its C-terminal domain (residues 94−354) is globular, is highly helical, and has a fold similar to that of glutathione *S*-transferases (GSTs) (*13*, *14*). This domain complements *URE2* gene deletion and is therefore considered as the functional domain of the protein (*10*). The N-terminal domain of the protein (residues 1−93) has an unusual content with a high proportion of four amino acid residues (asparagine, glutamine, serine, and threonine, 35%, 10%, 12%, and 5%, respectively). It is poorly structured (*12*) and required for the propagation of the prion phenotype (*10*, *15*). It is therefore referred to as the prion forming domain (PFD).

Purified, recombinant Ure2p oligomerizes in vitro into high molecular mass species that are ring-shaped in the early stages of assembly and fibrillar later on (*12*, *16*). The assembly reaction is accompanied by an increased binding of the dyes Congo Red and thioflavin T and an increased resistance to proteolysis (*12*, *16*, *17*). Strikingly however, while Congo Red binding is accompanied by the yellow-

† This work was funded by the French Ministry of Research and Technology and the Centre National de la Recherche Scientifique.

* Corresponding authors. E-mail: melki@lebs.cnrs-gif.fr and redeker@lebs.cnrs-gif.fr. Tel: 33 169823503. Fax: 33 169823129.

‡ The first two authors contributed equally to this work.

§ Laboratoire d'Enzymologie et Biochimie Structurales, CNRS.

|| Present address: EMBL, 6 rue Jules Horowitz, BP181, 38042 Grenoble Cedex 9, France.

⊥ Institut de Biochimie, Université Paris-Sud.

10.1021/bi049828e CCC: $27.50
Published on Web 04/03/2004

green birefringence in cross-polarized light, a property widely believed to be characteristic of amyloids, suggesting that the assembly reaction is driven by a major conformational change, the degradation patterns of soluble and assembled Ure2p are very similar, suggesting that assembly is instead driven by subtle rearrangements similar to those at the origin of the assembly of biological polymers (*18*, *19*) or that of proteins involved in conformational diseases (*20*, *21*). We recently demonstrated using FTIR spectroscopy and X-ray fiber diffraction that Ure2p fibrils assembled under physiologically relevant conditions lack the cross-β-structure of amyloids (*16*, *22*). A working model for fibril formation, based on the assembly of native-like molecules driven by non-native interactions between the N- and C-terminal domains of the protein was proposed (*16*). An alternative model for the assembly of Ure2p into fibrils, based on the stacking of Ure2p N-terminal domains into a central cross-β-core running all along the fibrils from which the C-terminal domains protrude, has been proposed (*23*, *24*).

To better understand the molecular events that lead to the assembly of Ure2p into protein fibrils, it is crucial to further document the structure of Ure2p in the fibrillar scaffold. Here we show that Congo Red binding and the associated yellow-green birefringence in cross-polarized light are not specific of amyloids. We also demonstrate by a combination of biochemical and biophysical approaches performed on the soluble and assembled forms of Ure2p among which proteolytic treatments, a straightforward method to probe the accessibility and the plasticity of proteins, SDS−PAGE analysis coupled to the identification of all cleavage sites by Edman sequencing, and MALDI-TOF mass spectrometry that the N-terminal domain of Ure2p is not fully protected against limited proteolysis in Ure2p fibrils. Finally, we demonstrate that the C-terminal domain of the protein is involved in the fibrillar scaffold. Our results are incompatible with the model where the N-terminal domains of Ure2p form a central cross-β-core running all along the fibrils from which the C-terminal domains protrude and bring novel insight in the process of Ure2p assembly into protein fibrils.

EXPERIMENTAL PROCEDURES

Protein Purification. Recombinant full-length Ure2p (Ure2p 1−354) was overexpressed as soluble proteins in *Escherichia coli*, purified as previously described (*12*, *25*), and stored at −80 °C in buffer A (20 mM Tris-HCl,[1] pH 7.5, 250 mM KCl, 1 mM DTT, 1 mM EGTA) at a concentration of 10 mg/mL. Actin was purified from rabbit muscle acetone powder (*26*, *27*) and stored as Ca-ATP−G-actin at 4 °C as described (*28*) following gel filtration chromatography (*29*). Pure tubulin was prepared from fresh pig brains as previously described (*30*, *31*) and stored at −80 °C (*28*).

Construction of the Ure2pI91EGR94 Variant Expression Vector in E. coli. The variant Ure2pI91EGR94 expression vector was obtained by site-directed mutagenesis by replacing the 5′-TTTTCGGATATG-3′ codons encoding F91, S92, D93, and M94 residues by 5′-ATTGAGGGTCGTAGT-3′ codons encoding I91, E92, G93, and R94. Mutagenesis was achieved in pET-URE2 expression (*25*) vector using the QuickChange site-directed mutagenesis kit (Stratagene Europe, Amsterdam, The Netherlands) and the primers 5′-CGACAACAACAACAGGCAATTGAGGGTCGTAGTC-ACGTGGAGTATTCC-3′ and 5′-GGAATACTCCACGTGA-CTACGACCCTCAATTGCCTGTTGTTCTCG-3′.

Assembly of Ure2p into Fibrils. The assembly of full-length wild-type Ure2p and the Ure2pI91EGR94 variant was achieved by incubation of the protein (50−100 μM) at 4 °C without shaking for 4−7 days in buffer A. The assembly reaction was monitored using thioflavin T binding (*32*) using a Quantamaster QM 2000-4 spectrofluorometer (Photon Technology International, Inc., Laurenceville, NJ). Ure2p fibrils were also examined following negative staining with 1% uranyl acetate on carbon-coated grids (200 mesh) in a Philips EM 410 electron microscope (Philips Inc., Amsterdam, The Netherlands).

Congo Red Binding Assay. The Congo Red (Sigma, Sigma-Aldrich Corp., St. Louis, MO) concentration was adjusted to 50 μM in solutions of preassembled Ure2p fibrils (50 μM in buffer A), actin filaments (50 μM G-actin in 5 mM Tris-HCl, pH 7.8, 0.1 M KCl, 0.2 mM DTT, 0.1 mM $CaCl_2$, 0.2 mM ATP, 2 mM $MgCl_2$, 100 μM phalloidin), and microtubules (75 μM tubulin in 0.05 M MES, pH 6.8, 0.5 mM EGTA, 6 mM $MgCl_2$, 1 mM GTP, 75 μM taxol, assembled at 30 °C). The polymers were then sedimented at 20 °C in a TL100 Tabletop Beckman ultracentrifuge (Beckman Instruments, Inc., Fullerton, CA) at 25000*g* for 30 min. A proportion of Ure2p fibrils and actin filaments remain in the supernatant following this centrifugation step. The samples were therefore further spun at 200000*g* for 20 min. The pellets were washed four times using an equal volume of water. Following resuspension of the pellets an aliquot was placed on a glass coverslip and allowed to dry. Excess Congo Red was removed with 90% ethanol (*17*), and the dried aliquots were viewed in bright field and cross-polarized light by polarization microscopy using a Leica (MZ12.5) microscope equipped with cross-polarizers (Leica Microsystems, Ltd., Heerbrugg, Switzerland).

Proteolytic Treatments of the Soluble and Assembled Forms of Ure2p. Soluble and fibrillar wild-type Ure2p were subjected to proteolysis using trypsin, chymotrypsin, or proteinase K at a weight ratio of 1:5800, 1:1000, and 1:10000, respectively. All of the proteases were purchased from Roche (Roche Diagnostics GmbH, Mannheim, Germany). The digestion of Ure2p (1 mg/mL) was carried out at 37 °C in buffer (20 mM Tris-HCl, pH 7.5, 25 mM KCl, 0.2 mM DTT, 0.2 mM EGTA). Aliquots were removed in duplicate after various time intervals. The reaction was stopped simultaneously by addition of PMSF (to a final concentration of 1 μM) or trifluoroacetic acid (to a final concentration of 1%) for SDS−PAGE and MALDI-TOF MS analysis, respectively. The samples devoted to SDS−PAGE analysis were immediately mixed (1:1 volume ratio) with denaturing buffer (50 mM Tris-HCl, pH 6.8, 4% SDS, 2% β-mercaptoethanol, 12% glycerol, 0.01% bromophenol blue) preheated at 95 °C and further incubated at the same temperature for 10 min. The aliquots containing 1% trifluo-

[1] Abbreviations: DTT, dithiothreitol; EGTA, ethylene glycol bis-(β-aminoethyl ether)-*N*,*N*,*N*′,*N*′-tetraacetic acid; ATP, adenosine 5′-triphosphate; GTP, guanosine 5′-triphosphate; MES, 2-(*N*-morpholino)-ethanesulfonic acid; Tris, tris(hydroxymethyl)aminomethane; PMSF, phenylmethanesulfonyl fluoride; DHB, 2,5-dihydroxybenzoic acid; CHCA, α-cyano-4-hydroxycinnamic acid; sinapinic acid, 3,5-dimethoxy-4-hydroxycinnamic acid; PVDF, poly(vinylidene difluoride).

roacetic acid were mixed to the suitable matrix solution and processed for mass spectrometry analysis.

Cleavage of the Ure2pI91EGR94 variant by the restriction protease factor Xa (Roche Diagnostics GmbH, Mannheim, Germany) was performed following the manufacturer's recommendations.

MALDI-TOF Mass Spectrometry Analysis. Soluble and fibrillar Ure2p and their respective fragments were subjected to MALDI-TOF analysis. All samples were prepared in triplicate using three different matrices: DHB, CHCA, and sinapinic acid (Aldrich Chemical Co. Inc., Milwaukee, WI). DHB and CHCA matrices were used for small fragment (up to 5−5 000 Da) mass determination using the reflectron mode. The sinapinic acid matrix was used for longer, mostly partially cleaved, fragments, from 5 to 40 kDa. The spectra were acquired on a MALDI-TOF mass spectrometer (Voyager Elite; Perseptive Biosystems, Inc., Framingham, MA) equipped with a nitrogen laser beam (337 nm) and a delayed extraction device. MALDI-TOF MS was performed in linear and reflectron modes to cover a mass range from 600 to at least 15000 Da. In the positive and linear mode, the accelerating voltage was 20 kV, the grid voltage 93%, and the delayed extraction 300 ns, while in the reflectron mode the accelerating voltage was 25 kV, the grid voltage 73%, and the delayed extraction 200 ns. About 200 shots were averaged for each acquired spectrum. Mass calibration was achieved using enolase, carbonic anhydrase, cytochrome *c*, ACTH (*7*−*38*), ACTH (*18*−*39*), ACTH (*1*−*17*), neurotensin, Tyr8-Substance P, and des-Arg-bradykinin. In the reflectron mode, the resolution was about 5−10000 in the range from 600 to 6000 Da, with an accuracy lower than 50 ppm. In the linear mode, the difference between the calculated average mass and the experimental mass determination of 0.05% is consistent with the accuracy of MALDI-TOF mass spectrometry.

SDS−*PAGE Electrophoresis and Western Blotting.* SDS−polyacrylamide gel electrophoresis was performed in 12% and 15% polyacrylamide gels (14 × 15 × 0.15 cm) following the standard method described by Laemmli (*33*). To sequence the proteolytic products observed on the SDS gels, the polypetides were transferred onto PVDF membranes following the manufacturer's recommendations (User bulletin 58, Dec 1993, PE Applied Biosystems). Duplicate gels, ran in parallel, were stained either with Coomassie blue or with silver nitrate (*34*). Following destaining, the gels were imaged using a CCD camera (Sony Corp., Tokyo, Japan) and further analyzed on a MacIntosh (Apple Computer, Inc., Cupertino, CA) computer using the software NIH Image (developed at the National Institutes of Health and available on the Internet at http://rsb.info.nih.gov/nih-image/).

Protein Sequencing. Peptide sequence data for full-length Ure2p as well as Ure2p fragments were obtained by automated Edman degradation using a sequencer (Applied Biosystems, Inc., Foster City, CA) equipped with an online phenylthiohydantoin amino acid analysis system (model 120A; Applied Biosystems, Inc.).

RESULTS

Binding of Congo Red to Ure2p Fibrils and the Associated Yellow-Green Birefringence in Polarized Light Are Not Indicative That the Polymers Are Amyloids. Ure2p fibrils assembled under physiologically relevant conditions have many properties akin to amyloids: among these properties, the binding of Congo Red and the associated yellow-green birefringence in polarized light (*12*, *17*, *25*). Although binding of Congo Red is not specific of amyloids (*35*, *36*), the associated yellow-green birefringence in polarized light is still considered by a number of authors as the signature of the high cross-β-structure content of Ure2p fibrils (*24*). Thus, although lacking (i) bands typically expected for the cross-β-structure (e.g., bands at 1623−1618 cm^{-1}; *37*) (*16*) and (ii) the 4.7 Å reflection in X-ray diffraction images (*38*) characteristic of amyloids (*22*), Ure2p fibrils are still considered to be amyloids (*24*). To determine whether binding of Congo Red to Ure2p fibrils assembled under physiologically relevant conditions and the associated yellow-green birefringence are meaningful, we compared the dye binding properties of Ure2p to those of other biological polymers, namely, actin filaments and microtubules, where high-resolution models of the assembled forms of the protein are available, demonstrating the absence of cross-β-structures (*18*, *19*). Figure 1A shows the binding of Congo Red to Ure2p fibrils, actin filaments, and microtubules using a sedimentation assay. Binding of Congo Red to all of these polymers is accompanied by yellow-green birefringence in polarized light as shown in Figure 1B. We conclude from this observation that the yellow-green birefringence observed upon Congo Red binding to highly ordered polymers cannot as such be considered as characteristic of amyloids.

Limited Proteolysis of Full-Length Soluble Ure2p. Limited proteolysis is a powerful tool for investigating protein structure, in particular, flexible regions and loops from folded polypeptide chains exposed to the solvent. Indeed, among all potential cleavage sites predicted by primary structure analysis for one given protease, only a few are found to be sensitive to limited proteolysis. This finding has been attributed to the backbone accessibility and its distortion capacities.

Figure 2 shows the potential cleavage sites along the primary structure of Ure2p of three different proteases: one with very narrow, a second with loose, and a third with broad specificity requirements, namely, trypsin, chymotrypsin, and proteinase K, respectively. Only a subset of the 145, 80, and 29 potential cleavage sites for proteinase K, chymotrypsin, and trypsin, respectively, are accessible under limited proteolysis conditions. The identification of the different polypeptides generated upon cleavage of Ure2p by these proteases with molecular masses ranging from 90 to 40328 Da is a complex issue as their theoretical number depending on whether miscleavage and methionine oxidation occurs is 36234, 10000, and 1800 for proteinase K, chymotrypsin, and trypsin, respectively.

The experimental conditions for limited proteolysis using the three enzymes listed above were determined by analyzing the onset of Ure2p cleavage reaction by SDS−PAGE and MALDI-TOF MS. As shown earlier (*12*), Ure2p cleavage is a progressive process. To favor the accumulation of Ure2p degradation products over time and to obtain reproducible limited proteolysis patterns, fixed enzyme-to-protein ratios were used after preliminary experiments where the enzyme-to-protein ratios varied from 1:500 to 1:200000. The best data, shown on the SDS−PAGE in Figure 3, were obtained using the following enzyme-to-protein ratios: 1:5800, 1:1000,

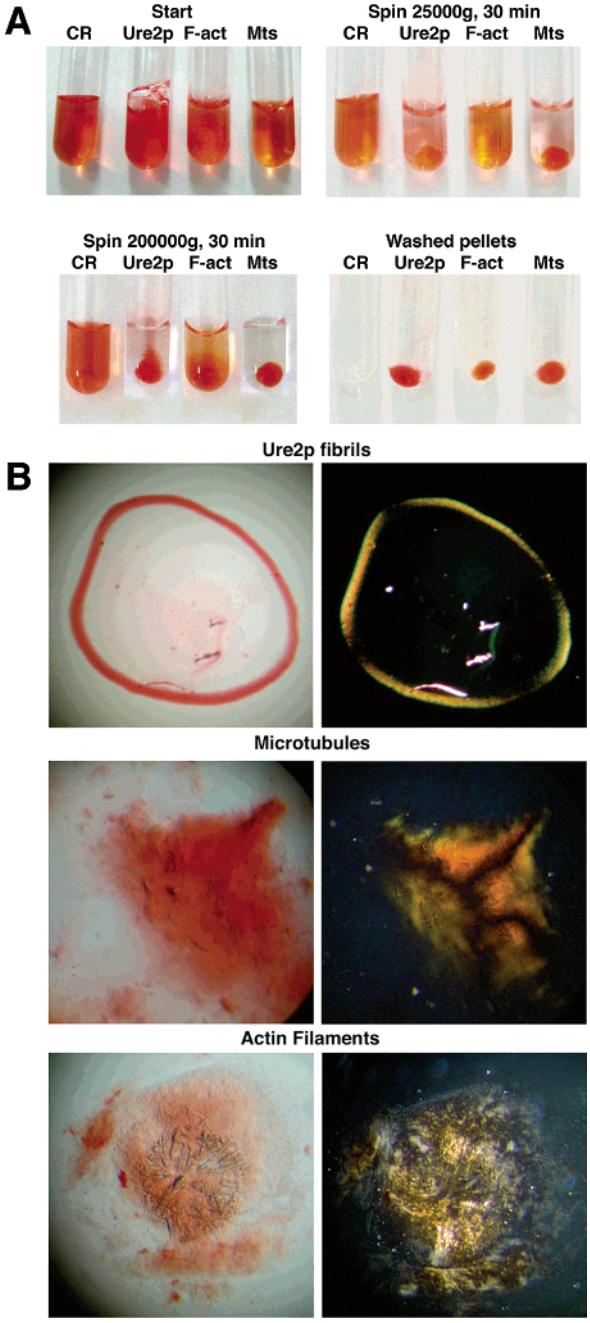

FIGURE 1: Congo Red binding to assembled Ure2p and the associated yellow-green birefringence in polarized light are not indicative that Ure2p fibrils are amyloids. (A) Sedimentation assay showing the binding of Congo Red to Ure2p fibrils, actin filaments, and microtubules. Congo Red (50 μM) was added to buffer A (control reaction) and to solutions containing preassembled Ure2p fibrils (50 μM), actin filaments, and microtubules in the buffers indicated in Experimental Procedures (upper left panel). The solutions were then centrifuged at 25000*g* for 30 min at 20 °C (upper right panel). Fibrils are still present in the supernatant of the tubes containing Ure2p and filamentous actin. The same tubes were further spun at 200000*g* for 20 min at 20 °C (lower left panel). The pellets were washed four times with water and suspended in 20 μL of water (lower right panel). (B) Binding of Congo Red to Ure2p fibrils, actin filaments, and microtubules is accompanied by yellow-green birefringence. A dried aliquot of each suspension was washed with ethanol, and the polymers were visualized in bright (left panels) and cross-polarized light (right panels).

and 1:10000 for trypsin, chymotrypsin, and proteinase K, respectively.

The separation of proteolytic products of Ure2p on SDS−PAGE coupled to the N-terminal amino acid sequencing of the polypeptide chains generated allowed the identification of accessible cleavage sites. It also allowed us to draft a comprehensive picture of the cleavage reaction from both the time course of the cleavage reaction and the relative intensities of the polypeptides generated.

In our hands, the separation of the proteolytic fragments generated upon treatment of Ure2p with the different proteases by reversed-phase HPLC proved difficult to achieve and was potentially biased because of (i) the difficulties encountered when trying to fully dissolve the assembled form of Ure2p in the absence of SDS, (ii) the overlap between different peaks due to the large number of proteolytic products, and (iii) the high risk of selecting or enriching artificially a subset of peptides. We therefore used MALDI-TOF MS that allows the analysis of mixtures of peptides and proteins over a broad mass range with high sensitivity and a high tolerance for contaminants (buffer, salts, some detergents) to analyze directly the complex peptide mixtures obtained upon proteolytic treatment of the soluble and assembled forms of Ure2p. The kinetic analysis of the polypeptides generated by the cleavage reactions allowed us to observe their accumulation and decrease over time but not their quantification.

Trypsin cleaves rapidly (in less than 1 min) soluble wild-type Ure2p at positions R17, R24, and R65 (Figure 3A). Later on, at time 5 min, cleavage occurs at positions R101 and K104 with high efficiency as compared to cleavage at position R85. Polypeptides 18−354 and 25−354 accumulate up to 2 h. A shorter polypeptide extending from amino acid residue 105 to amino acid residue 354 is generated after incubation of Ure2p in the presence of trypsin for 30 min. This fragment resists the tryptic treatment for over 24 h. It therefore constitutes a compact, highly resistant part of the protein, in agreement with previous observations (*12*). Upon incubation of Ure2p in the presence of trypsin for over 24 h, polypeptide 153−354 is generated. The latter cleavage site is located in a region exposed to the solvent according to the three-dimensional structure of Ure2p 95−354 (*13*). This region is probably flexible and, thus, accessible to the protease. Interestingly, cleavage does not occur at the potential cleavage site K78, suggesting that this amino acid residue is located in a structured region extending from residue N66 to residue R85, including the latter residue as witnessed by the low efficiency of cleavage at position R85.

The first peptide detected after 1 min digestion by MALDI-TOF MS corresponds to the peptide 1−17 (Figure 4A). This clearly indicates that the first tryptic cleavage event occurs at position R17. At time point 5 min, efficient cleavage occurs at residues R24 and R65 while cleavage at residues R85 and R101 is less efficient. Two hours after the onset of the cleavage reaction, polypeptides 18−65, 25−65, 66−101, and 66−104 accumulate, in agreement with what is expected from SDS−PAGE and Edman degradation analysis. Interestingly, the potential polypeptides 79−101, 79−104, and 79−85 are not detected 2 h following the onset of the tryptic treatment. We conclude from this observation and the Edman degradation results that the potential cleavage site at residue K78 is located in a potentially ordered structure.

Treatment of Ure2p by chymotrypsin for 5 min yields polypeptides with apparent molecular masses of 39 and 29

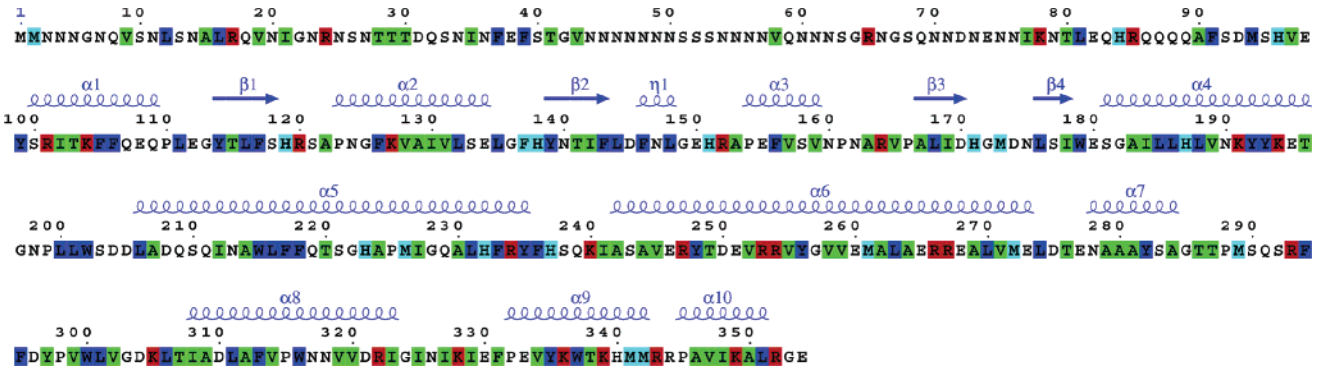

FIGURE 2: Potential cleavage sites along the primary structure of Ure2p of the proteases used in this work. Predictions of the potential cleavage sites of trypsin (red), chymotrypsin (blue and cyan), and proteinase K (blue and green) were obtained through the peptidecutter software (http://us.expasy.org/tools/peptidecutter/). Cleavage sites common to chymotrypsin and proteinase K are in blue. The secondary structure content of Ure2p (*13*) is represented above the primary structure. The figure was created using ESPript (*48*).

kDa on SDS−PAGE and the N-terminal amino acid residues S13 and R17 for the 39 kDa polypeptide and S92, S100, and F106 for the 29 kDa product (Figure 3B). The N-terminal amino acid residue of the fragment with an apparent molecular mass of 33 kDa corresponds to that of intact Ure2p, which indicates that cleavage occurs within the globular C-terminal domain of the protein potentially within the highly flexible region extending from amino acid residue 280 to amino acid residue 300, the α-cap region (*13*). While the 29 kDa product is degraded, three polypeptides are produced and accumulate for over 2 h. They have apparent molecular masses of 20, 19, and 7−10 kDa and the N-terminal amino acid residues S100, F106, and S283, respectively. The concomitant disappearance of the 29 kDa degradation product and generation of the 19 and 7−10 kDa polypeptides suggest that they result from cleavage of the 29 kDa polypeptide in the α-cap region mentioned above at amino acid residue Y282. The 19 and 7−10 kDa polypeptides resist chymotryptic treatment for over 4 h although containing a large number of potential cleavage sites. This could be in part due to their location at the interface between the two monomers in the Ure2p dimer.

MALDI-TOF MS analysis reveals that five polypeptides are generated within the first minute of chymotryptic treatment (Figure 4D). Four come from cleavage occurring within the N-terminal domain of the protein (polypeptides 1−16, 1−37, 1−91, and 1−99) and one (polypeptide 283−354) from within the α-cap region. Five minutes after the onset of the proteolytic treatment additional polypeptides coming mainly from cleavage reactions occurring at amino acid residues L12, F39, F105, and F294 are detected. Later on, at time point 10 min, cleavage occurs at amino acid residue L81. We conclude from these observations and that obtained using trypsin that the N-terminal part of Ure2p extending up to residues 105 is highly flexible with the noticeable exception of the amino acid stretch 66−85.

The cleavage sites in the C-terminal domain of Ure2p identified by MALDI-TOF MS analysis were in accord with the structure of the protein (*13*) with all cleavage sites being exposed to the solvent. Cleavage occurred at amino acid residues F117 and F294 at time point 5 min, F146, F236, L186, and Y192 at time point 10 min, and Y256 and L231 at time points between 30 min and 2 h as shown in Figure 4F.

Finally, Ure2p was subjected to limited proteinase K treatment. Because of its broad cleavage specificity requirement, this enzyme allows the identification of the most flexible regions in Ure2p on one hand; however, for the same reason, a very large number of degradation products are generated, thus increasing significantly the complexity of the polypeptide identification process, in particular, that using MALDI-TOF MS.

The first polypeptide generated upon treatment of soluble full-length Ure2p for 0.5−1 min by proteinase K (Figure 3C) has an apparent molecular mass of 39 kDa on SDS−PAGE and the N-terminal amino acid residues S13 and R17. Later on, at time point 3 min, three polypeptides with apparent molecular masses 35, 33, and 31 kDa and the N-terminal amino acid residues T28, I35, and F37, respectively, are observed.

These products do not populate, which suggests that they are further degraded rapidly. As early as 1 min following the onset of the cleavage reaction, a polypeptide with an apparent molecular mass of 29 kDa and the N-terminal amino acid residues S92, S95, and K104 was observed. This large polypeptide reported previously upon treatment of Ure2p by proteinase K (*12*) accumulates during the first 10 min of proteinase K treatment and is further degraded later on.

Additional polypeptides are generated following the incubation of Ure2p with proteinase K for 30 min to 2 h. The major polypeptides have apparent molecular masses of 18 and 16 kDa and the N-terminal amino acid residue K104. It is reasonable to consider that these polypeptides originate from the cleavage of the 29 kDa polypeptide following an additional cleavage in the α-cap region as they accumulate upon degradation of the 29 kDa polypeptide. The observed difference in their apparent molecular masses is probably due to cleavage at two different sites within the α-cap region. A fuzzy band with an apparent molecular mass of 7−10 kDa that resists proteinase K treatment for over 2 h is generated in a synchronous manner. The identification by Edman degradation of these polypeptides revealed that they all originate from the C-terminal part of the protein as their N-terminal amino acid residues are S283, G285, W300, and L301, clearly demonstrating that cleavage occurs within two amino acid residue clusters in the highly flexible α-cap region. Thus the 29 kDa polypeptide representing the globular C-terminal domain of Ure2p appears indeed to be

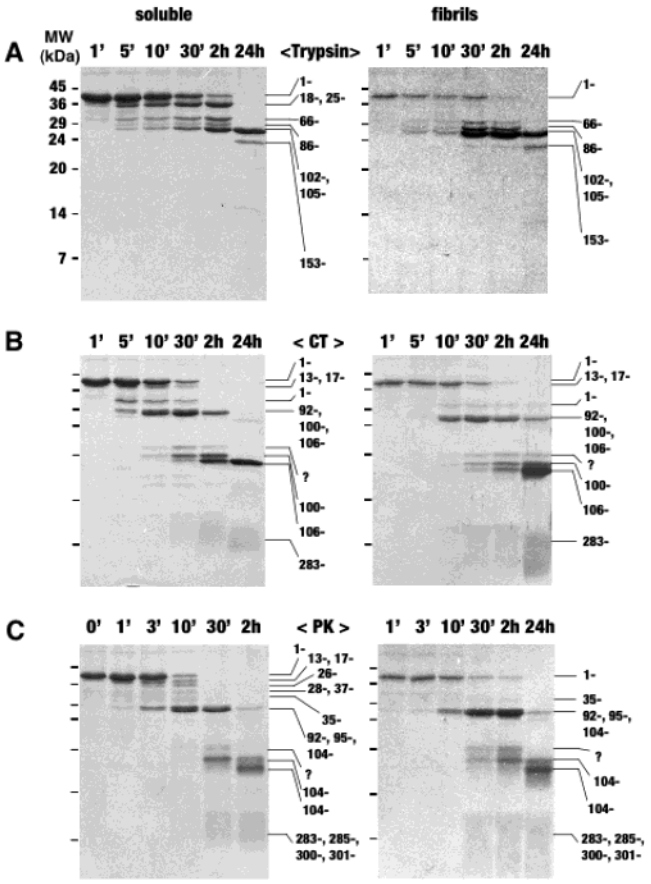

FIGURE 3: Identification of the reaction products of the proteolytic treatment of the soluble and assembled forms of Ure2p. The time courses of degradation of the soluble (left panels) and assembled (right panels) forms of Ure2p (1 mg/mL) by trypsin (0.17 μg/mL) (A), chymotrypsin (1 μg/mL) (B), and proteinase K (0.1 μg/mL) (C) were monitored by SDS−PAGE. Ure2p cleavage reactions were stopped at the time points indicated on the top of each gel by addition of PMSF (1 μM) and preheated denaturing buffer to the aliquots. Two 12% polyacrylamide gels were run in duplicate: one was stained with Coomassie blue, and the other was transferred on a PVDF membrane for N-terminal amino acid sequencing of at least five residues of each polypetide band after Coomassie blue staining. The position of the N-terminal amino acid residue identified by Edman degradation for each polypeptide band is indicated between the panels corresponding to the degradation reactions by each protease of the soluble and assembled forms of Ure2p. The molecular mass markers are shown on the left.

cleaved into two byproducts with apparent molecular masses of 16 and 7−10 kDa.

Altogether, our results reveal the existence of hot spots for proteolytic cleavage in Ure2p. The N-terminal domain as a whole is fully accessible to proteolysis with the exception of the amino acid stretch 66−81 and possibly 85. The latter strongly suggests the existence of structured regions within the supposedly fully unfolded N-terminal domain of Ure2p. The second hot spot is located between amino acid residues 86−117. This region appears as a 31 amino acid residue flexible region linking the globular and the prion-forming domains of Ure2p. The third and last hot spot for proteolytic cleavage in Ure2p lies within the α-cap region extending from amino acid residue S283 to amino acid residue L301. It is interesting to note that cleavage of Ure2p within the α-cap region has no significant influence on the overall tertiary and quaternary structures of soluble dimeric Ure2p as observed upon comparing the three-dimensional structures of Bousset et al. (*13*) and Umland et al. (*14*).

Changes in the Cleavage Pattern of Full-Length Ure2p upon Assembly into Protein Fibrils. To determine whether Ure2p assembly is accompanied either by a conformational change or by an increased protection toward proteolysis of a region of the protein, fibrillar Ure2p was subjected to the same proteolytic treatment as the soluble form, and the time course of cleavage was analyzed by SDS−PAGE and MALDI-TOF MS. The digestion profiles of the fibrillar form of Ure2p generated upon trypsin, chymotrypsin, and proteinase K digestions are shown in panels A, B, and C of Figure 3, respectively. The polypeptide bands were identified by Edman degradation and MALDI-TOF MS as for soluble Ure2p.

Overall, the quantitative comparison of the SDS−PAGE profiles obtained for the soluble and the fibrillar forms of Ure2p shows that the cleavage rate decreases upon assembly of Ure2p. In addition, while all of the degradation products with molecular masses below 30 kDa are generated, several polypeptides with molecular masses between 38 and 30 kDa are either poorly populated or not observed, indicating that a number of potential cleavage sites located within the N-terminal part of the protein are less exposed to the solvent. Indeed, SDS−PAGE analysis reveals that the polypeptides with the N-terminal amino acid residues Q18 and N25, S13, and R17, and S13, R17, and S26, generated upon treatment of the soluble form of Ure2p by trypsin, chymotrypsin, and proteinase K, respectively, are absent from the degradation profiles of the fibrillar form of the protein.

These observations are further supported by the MALDI-TOF MS analysis where polypeptides 1−17 and 1−24 were detected in trace amounts or not at all, respectively, in the tryptic digest of assembled Ure2p. Similarly, polypeptides 1−12, 1−17, 13−91, and 17−91 were not detected upon treatment of assembled Ure2p by chymotrypsin. Most interestingly, MALDI-TOF analysis allowed the identification of cleavage sites that are significantly more exposed to the solvent in the assembled form of the protein as compared to soluble Ure2p. Indeed, trypsin was found to cleave with higher efficiency at the early stages of the proteolytic treatment (e.g., at time points 5 and 10 min) at amino acid residues R65 and R85, yielding larger amounts of polypeptides 66−101, 66−104, 66−85, 86−101, and 86−104.

In the presence of chymotrypsin, polypeptides 40−91, 38−91, and 40−99 are detected, indicating that cleavage sites at amino acid residues F37 and F39 are exposed to the solvent in fibrillar Ure2p. Furthermore, and in agreement with data obtained with trypsin, chymotrypsin was found to cleave with higher efficiency the fibrillar form of Ure2p at amino acid residue L81, yielding polypeptide 82−146.

Comparison of the polypeptides generated upon treatment of fibrillar Ure2p by trypsin or chymotrypsin clearly indicates that the cleavage sites located in the region extending from amino acid residue 12 to amino acid residue 38 are significantly protected toward proteolysis. Another stretch of amino acids is significantly protected within the fibrils. Indeed, the chymotrypsin cleavage sites located in the flexible α-cap region appear also to be protected as well. While the 33 kDa fragment corresponding to Ure2p cleaved in the α-cap region with an intact N-terminal is degraded within 10 min in soluble Ure2p, this polypeptide resists

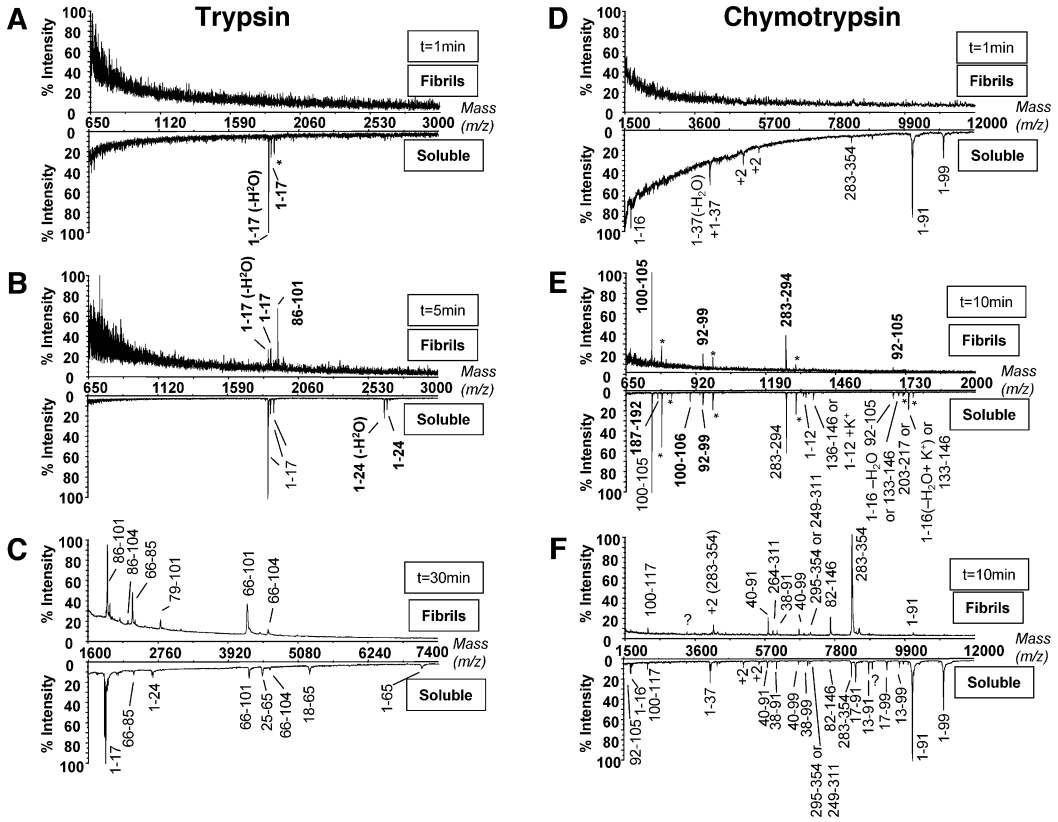

FIGURE 4: Susceptibility to proteolysis of a number of cleavage site changes upon assembly of Ure2p into protein fibrils. The soluble and assembled forms of full-length Ure2p were subjected to limited proteolysis with trypsin (A−C) and chymotrypsin (D−F). The time course of reaction product generation was analyzed by MALDI-TOF mass spectrometry. The time points are 1 min in panels A and D, 5 min in panel B, 10 min in panels E and F, and 30 min in panel C. Peptides present in the digestion mixture were analyzed in the reflectron mode in panels A, B, and E and in the linear mode in panels C, D, and F. Each peak is labeled with the peptide to which it corresponds. Biprotonated ions are labeled (+2). Unidentified peptides are labeled with a question mark (?), and potassium ion adducts are labeled with an asterisk (*).

proteolysis for over 24 h in the assembled form of the protein, suggesting a significant protection of the C-terminal domain of Ure2p within the fibrils.

It is worth noticing that treatment of fibrillar Ure2p by chymotrypsin and proteinase K yields polypeptides with apparent molecular masses of 7−10 kDa in a manner similar to what is observed upon treatment of soluble Ure2p with the same proteases. Edman degradation of this polypeptide species, together with MALDI-TOF MS analysis, demonstrates that it originates from the C-terminal part of Ure2p with (i) the N-terminal amino acid residues S283, G285, W300, and L301 and (ii) a molecular mass of 8500.

The Globular C-Terminal Domain of Ure2p (Ure2p 94−354) Is Tightly Involved in the Fibrillar Scaffold. The treatment of filamentous Ure2p by proteinase K has been reported recently to yield thin fibrils made of polypeptides originating from the N-terminal domain of the protein that are 4 nm wide (*24*). These highly resistant fibrils can be separated by ultracentrifugation from polypeptides originating from the C-terminal domain of Ure2p that is cleaved by proteinase K into small soluble polypeptides (*24*). These data strongly support a model where the N-terminal domains of Ure2p constitute the backbone of the filaments while the surrounding C-terminal moieties of the protein are not tightly involved in the fibrillar scaffold. Using AFM imaging and electron microscopy, we reported that treatment of Ure2p fibrils in solution by proteinase K is not sufficient to disrupt the fibrillar structure but leads instead to a reduction of fibril rigidity (*16*). On the basis of this observation we hypothesized that Ure2p 95−354 is involved in the fibrillar scaffold. To determine whether Ure2p 95−354 surrounds the N-terminal moiety of the protein or is involved in the fibrillar scaffold, i.e., whether it is released in the medium or remains associated to the fibrils upon cleavage between the N- and C-terminal moieties of the protein, we engineered a highly specific cleavage site between these moieties as described in Experimental Procedures. The variant Ure2pI91EGR94 assembles in vitro into fibrils that are indistinguishable in the electron microscope from fibrils made of wild-type full-length Ure2p (Figure 5A,B). Treatment of preassembled Ure2pI91EGR94 fibrils with the site-specific protease factor Xa has no effect on the shape of the fibrils (Figure 5C) and yields, as expected, two polypeptides with apparent molecular masses 30 and 10 kDa corresponding to Ure2p 95−354 and 1−91, respectively. SDS−PAGE analysis of the polypeptide content of the pellet and the supernatant fractions of sedimented Ure2pI91EGR94 fibrils treated by factor Xa strongly suggests either that Ure2p 95−354 is involved in the fibrillar scaffold or that it interacts strongly with the N-terminal domain of the protein as the polypeptides cosediment (Figure 5D). To distinguish between these two possibilities, Ure2pI91EGR94 fibrils pretreated by factor Xa were incubated for 1 h at 20 °C in the presence of 4 M GdnHCl prior to their sedimentation. Figure 5E clearly demonstrates that the interaction between the N- and C-terminal domains of Ure2p within the fibrils is not weakened

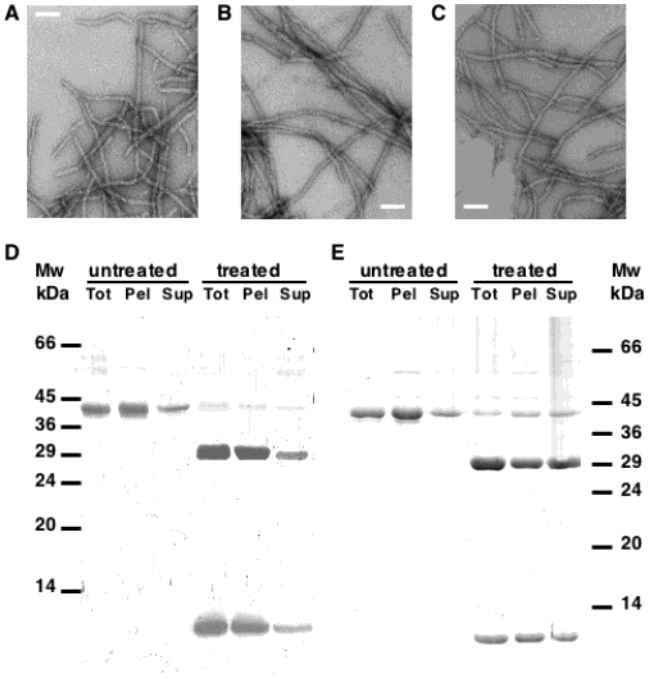

FIGURE 5: The globular C-terminal domain of Ure2p remains associated to the fibrils following treatment of the fibrillar form of the variant Ure2pI91EGR94 by the site-specific protease factor Xa. (A−C) Negative-stained electron micrographs of wild-type Ure2p and Ure2pI91EGR94 fibrils before and after treatment with factor Xa, respectively. Bar = 0.1 μm. (D) Ure2pI91EGR94 fibrils (2 mg/mL) in 20 mM Tris-HCl, pH 7.5, 50 mM KCl, 1 mM EGTA, and 1 mM DTT were spun at 100000*g* for 30 min at 15 °C either without any further treatment or following incubation with the site-specific protease (2.5 μg/mL) for 8 h, and the protein content in the pellet and supernatant fractions was analyzed by SDS−PAGE. To document the strength of the interaction between the N- and C-terminal domains of the protein within the fibrils, the GdnHCl concentration was adjusted to 4 M in solutions of untreated and factor Xa treated Ure2pI91EGR94 fibrils, and the samples were centrifuged for 3 h at 300000*g* and 15 °C to take into account the viscosity of the solution. (E) SDS−PAGE analysis of the protein content in the pellet and supernatant fractions of untreated and factor Xa treated Ure2pI91EGR94 fibrils in the presence of GdnHCl. The 12% polyacrylamide gels were silver stained. The molecular mass markers are shown.

by GdnHCl treatment as Ure2p 1−91 and 95−354 remain associated. We conclude from these findings that the domains of Ure2p remain associated within the fibrils following cleavage in the flexible region that bridges them together. The finding that the two domains of Ure2p cosediment even under denaturing conditions strongly suggests that the C-terminal domain of Ure2p is tightly involved in the fibrillar scaffold as the interaction between the two domains would have been suppressed as Ure2p 95−354 unfolds under the experimental conditions used (*25*, *39*).

DISCUSSION

Two models have been proposed to account for the assembly of Ure2p into protein fibrils and describe the architecture of the fibrils. The first model hypothesizes that the fibrils are amyloids. The assembly of the protein is according to this model driven by a conformational change of the N-terminal domain of the protein, leading to its organization into a cross-β-core running along the fibrils (*23*, *24*). This model is based on (i) the aspect of the fibrils (*12*, *17*), (ii) their ability to bind the dye Congo Red and exhibit a yellow-green birefringence in polarized light (*17*, *25*), (iii) their increased resistance to proteolysis (*12*), (iv) the persistence of a 4 nm residual filament after treatment of the fibrils with proteinase K (*17*, *24*, *40*), (v) the nature of the polypeptide that resists proteinase K treatment, (vi) the finding of β-sheet structure in mixtures containing Ure2p and a synthetic peptide reproducing the N-terminal 65 amino acids of Ure2p (*17*), (vii) the observation that the N-terminal 65 amino acids of Ure2p alone or fused to four different polypeptides form fibrils (*40*), (viii) the inaccessibility of the N-terminal domain of Ure2p to antibodies directed against the N-terminal moiety of the protein (*24*), and (ix) electron microscopy observations revealing the presence of a pattern compatible with a central backbone from which globular particles protrude (*24*).

The second model hypothesizes that the assembly of full-length Ure2p into fibrils is driven by limited conformational rearrangements and non-native inter- or intramolecular interactions between Ure2p monomers (*16*). This model is based on (i) the absence of a major conformational change as determined upon comparison of the proteolytic patterns and glutathione binding properties of the soluble and assembled forms of the protein (*12*), (ii) the observation that Ure2p fibrils assembled under physiologically relevant conditions are devoid of a cross-β-core as determined by FTIR spectroscopy and X-ray fiber diffraction images (*16*, *22*), and (iii) the finding that the fibrillar structure is not disrupted neither upon treatment of the fibrils by high concentrations of GdnHCl nor upon their complete digestion by proteinase K (*22*).

Significance of the Aspect of Ure2p Fibrils, Their Congo Red Binding Property, and the Associated Yellow-Green Birefringence in Polarized Light. Ure2p fibrils are about 20 nm wide and over 1 μm long. They are flexible and periodic. In that respect they resemble amyloids. Ure2p fibrils resemble as well a wide variety of biological polymers such as actin filaments that are 10 nm in diameter and over 1 μm long (*41*) and RecA and FtsZ fibrils that are 9 and 23 nm in diameter, respectively, and over 1 μm long (*42*, *43*). Ure2p fibrils are also very similar to protein involved in a number of diseases upon assembly into fibrils following subtle conformational changes such as lithostathine and the members of the serpin superfamily (*20*, *44*, *45*).

Congo Red binding is not specific of amyloids (*35*, *36*). It is, however, the yellow-green birefringence associated to Congo Red binding that is considered as one of the signatures of amyloids. We show here that biological polymers such as actin filaments and microtubules whose structures have been solved at an atomic resolution revealing the absence of a cross-β-core (*18*, *19*) bind Congo Red and exhibit yellow-green birefringence in polarized light upon staining.

Amyloids are defined as compact extracellular deposits with inherent birefringence associated to various pathologies and made of fibrillar materials that exhibit a typical cross-β-structure in X-ray fiber diffraction images (*5*, *46*). The inherent birefringence of amyloid deposits increases intensely upon binding of the dye Congo Red (*5*). Ure2p fibrils assembled in vitro under physiologically relevant conditions lack the typical cross-β-structure of amyloids (*22*). They are not associated to disease as yeast cells exhibiting the [URE3] phenotype grow relatively well. Finally, Ure2p deposits and

fibrils have been described as intracellular (*23*, *47*). Thus, it is crucial to avoid using the term amyloid and even amyloid-like when describing Ure2p fibrils based only on their congophilia and the associated yellow-green birefringence in polarized light.

Nature of the Polypeptide That Resists the Proteolytic Treatment of the Assembled Form of Ure2p. While the time courses of degradation of the soluble and fibrillar forms of Ure2p by a variety of proteases (trypsin, chymotrypsin, proteinase K, and subtilisin) differ significantly, the reaction products are very similar, suggesting that the overall conformation of Ure2p is not altered within fibrils assembled under physiologically relevant conditions (*12*). In contrast, the proteolytic pattern of Ure2p fibrils changes significantly upon the large structural rearrangement that occurs upon heat treatment of the fibrils (*22*). Based on polyclonal antibody recognition, on apparent molecular mass estimation from SDS−PAGE, and on mass spectrometry measurements, a 7−10 kDa polypeptide that resists significantly proteinase K treatment is proposed to represent a polypeptide from the N-terminal domain of Ure2p (*24*). The evidence that the 7−10 kDa polypeptide corresponds to the N-terminal domain of Ure2p is weak. Indeed, treatment of full-length soluble Ure2p and Ure2p 95−354 by proteinase K yields a polypeptide with the same apparent molecular mass (*25*). Furthermore, the polyclonal antibody that recognizes the N-terminal domain of Ure2p binds not only to purified full-length Ure2p but also to a polypeptide that has an apparent molecular mass of 7−10 kDa, which not only is present before the onset of the cleavage reaction (see lane 0 in Figure 3, lower panel, in ref *24*) but which does not appear to populate the mixture (compare the intensities in lanes 0 and 60 min in the same paper). Finally, the molecular masses of the polypeptides present in the proteinase K resistant fraction measured by LC-MS are 5744.5, 6042.5, 6171.2, and 6284.9. They were assigned to polypetides Q18−N70, V9−G64, Q8−G64 or S13−Q69, and G6−S63 or N7−G64 or L12−Q69, respectively, with an uncertainty of 0.2−1 Da (*24*). Proteinase K possesses 145 potential cleavage sites in Ure2p that could generate 36234 theoretical fragments ranging from 90 to 40328 Da. The number of polypeptides that can be theoretically generated upon proteinase K cleavage that have molecular masses of 5744.5 Da with a molecular mass uncertainty of ±1 Da is 11; that with a molecular mass uncertainty of ±2 Da is 20. This number increases considerably when the degree of oxidation of methionine residues is taken into account, which underlines the complexity and weakness of the assignment process of a measured molecular mass to a given polypeptide when proteinase K is used. To overcome this complexity, the fuzzy band on SDS−PAGE that resists significantly proteinase K and chymotrypsin treatments was subjected to Edman degradation. Our data demonstrate unequivocally that the polypeptides that constitute this band are generated following cleavage within the α-cap region that is located in the C-terminal domain of Ure2p.

Identification of Two Classes of Cleavage Sites in the N-Terminal Domain of Ure2p. The time-based comparison of the polypeptides generated upon cleavage of the soluble and assembled forms of Ure2p by trypsin and chymotrypsin by MALDI-TOF MS reveals the existence of two classes of cleavage sites within the N-terminal domain of Ure2p. The susceptibility to proteolysis of the first category is not significantly affected while that of the second category is either significantly increased or decreased. The first category is exemplified by cleavage following amino acid residues R65 for trypsin and F91 for chymotrypsin. The second class is exemplified by cleavage occurring at amino acid residues K78, R85, R17, and N23.

Comparison of the tryptic and chymotryptic polypeptides generated upon proteolytic treatment of the soluble and assembled forms of Ure2p reveals that the unique tryptic cleavage site located at amino acid residue R24, i.e., between amino acid residues 12 and 37 where cleavage occurs, is protected upon assembly of Ure2p. The finding that a 25 amino acid stretch at most is resistant to proteolysis, as compared to the 70 amino acid polypeptide proposed to constitute the cross-β-core of the fibrils (*24*), does not necessarily mean that it is involved in a cross-β-structure.

The Globular C-Terminal Domain of Ure2p Is Tightly Involved in the Fibrillar Scaffold. The cross-β-core model (*23*, *24*) predicts that the globular C-terminal domain of Ure2p should be released in the medium following specific cleavage between the N- and C-terminal domains of the protein in its fibrillar form. This is not what we observe upon cleavage between the two domains of Ure2p when the N-terminal domain of the protein is in its natural context in contrast with what occurs when it is fused to unrelated proteins such as GFP or barnase. The C-terminal domain of Ure2p is tightly bound to the high molecular mass fibrillar material even upon incubation of preformed fibrils treated by factor Xa in the presence of high GdnHCl concentrations. Thus the C-terminal domain of Ure2p is tightly involved in the fibrillar scaffold. This result is incompatible with the cross-β-core model (*24*) where the only part of Ure2p involved in the central cross-β-core, which runs all along the fibrils, is the flexible N-terminal domain of the protein with the globular C-terminal domain protruding from the polymers.

One obvious reason for the discrepancy between our results and those of Baxa and co-workers could be due to the experimental conditions used as our fibrils are assembled at pH 7.5 in the presence of KCl and without agitation while those of Baxa and co-workers are produced at pH 8.0 in the presence of NaCl and with agitation. We do not believe this is at the origin of the disagreement as the only difference we observe when the experimental conditions of Baxa and co-workers are used is a higher proportion of amorphous aggregates. The reason for the observed difference in our opinion is the use of the N-terminal domain of Ure2p out of its biological context. Indeed, it is reasonable to envisage that the N-terminal domain of Ure2p is not in the same conformation in a nonnatural context and in the authentic protein. The main evidence supporting this view is that full-length Ure2p assembles into fibrils with a lag phase of tens of hours while polypeptides reproducing the N-terminal 65−80 amino acid residues assemble into fibrils within minutes following dilution from denaturant. Other evidence for this view comes from the fact that while fibrils made of full-length Ure2p under physiologically relevant conditions lack both the FTIR spectroscopic and X-ray fiber diffraction signatures of cross-β-structures (*16*, *22*), mixed fibrils made of equimolar amounts of Ure2p 1−65 and full-length protein have an increased β-sheet content (*17*). This is typically what

is expected if Ure2p 1−65 was assembling β-rich structures while full-length Ure2p was assembling into fibrils where the native-like structure is maintained. The last evidence underlining the influence of the natural context of the N-terminal domain on the assembly reaction comes from Ure2p unfolding studies (*12*, *25*). The partial unfolding of Ure2p by GdnHCl leads to a significant reduction in its assembly capacities. If the flexible N-terminal domain of Ure2p was solely responsible for its assembly properties, the assembly reactions would be either unaffected or favored upon partial unfolding of the protein. Instead, amorphous aggregates are produced, thus indicating that the C-terminal domain of the protein is playing a central role in fibril formation.

Finally, the pattern observed on short stretches of Ure2p fibrils that has been attributed the role of the central cross-β-core (*24*) cannot be considered with confidence as such. Indeed, the observation of Ure2p fibrils by cryoelectron microscopy reveals either the absence of such pattern or the presence of one, two, and even three straight lines that can be considered as potential backbones of the fibril (Bousset and Melki, unpublished observations). These observations indicate some degree of variability in fibril morphology and a high degree of flexibility of the polymers. It is therefore crucial to reduce the heterogeneity of Ure2p fibrils and their flexibility using experimental conditions where the fibrils are either highly organized, e.g., with a pronounced helical twist, or very rigid to further improve the imaging resolution and build high-resolution three-dimensional maps of the fibrils. The latter will lead to a better understanding of the subtle conformational changes that are at the origin of Ure2p assembly into protein fibrils.

What is the extent of conformational change that accompanies the assembly of soluble Ure2p into fibrils? The answer to this question in the absence of three-dimensional reconstructions of Ure2p fibrils comes from the careful analysis of the cleavage reaction products of the soluble and assembled forms of the protein and their respective proportions that reflect differences in exposure to the solvent and accessibility to the proteases. It is crucial though to bear in mind during this exercise that a difference in accessibility of a given cleavage site may be the consequence of a conformational change such as a loop or α-helix to β-strand transition but also to molecular crowding. Our data clearly demonstrate that the cleavage site R24 located in the amino acid stretch L12−F37 is protected against cleavage in the assembled form of Ure2p. In contrast, the exposure to the solvent of the amino acid stretch R66−R86 increases upon assembly. The latter observation suggests that the flexible N-terminal domain is not fully unstructured. Indeed, cleavage sites located in the region extending from amino acid residue R66 to amino acid residue R86 are less exposed to the solvent and therefore more resistant to proteolysis in the soluble form of the protein. This region loses its structure and is exposed to the solvent upon assembly. This finding strongly suggests that the widely accepted view where the N-terminal domain of the Ure2p is very poorly structured should be revised. Further efforts to solve the three-dimensional structure of this domain in whole or in part should be attempted as this should lead to a better understanding of the mechanism of assembly of Ure2p in protein fibrils. Altogether, the data presented in this work are fully consistent with the model we proposed for the assembly of Ure2p into fibrils where assembly is driven by non-native inter- and/or intramolecular interaction between Ure2p monomers following subtle conformational changes (*16*) and reveal weaknesses in the cross-β-core model.

ACKNOWLEDGMENT

We thank Ludovic Guigou for help in bright field and cross-polarized light microscopy image acquisition and Christophe Marchand for help in mass spectrometry measurements. This work is dedicated to Dr. Jean Bousset.

SUPPORTING INFORMATION AVAILABLE

MALDI-TOF MS analysis of the time courses of cleavage of the soluble and assembled forms of Ure2p by trypsin (Figure I) and chymotrypsin (Figure II) and bright and cross-polarized light images of Ure2p fibrils, actin filaments, and microtubules stained by Congo Red and dried on a glass coverslip without further treatment with 90% ethanol (Figure III). This material is available free of charge via the Internet at http://pubs.acs.org.

REFERENCES

1. Prusiner, S. B. (1998) Prions, *Proc. Natl. Acad. Sci. U.S.A. 95*, 13363−13383.
2. Wickner, R. B. (1994) [URE3] as an altered URE2 protein: evidence for a prion analogue in *Saccharomyces cerevisiae*, *Science 264*, 566−569.
3. Coustou, V., Deleu, C., Saupe, S., and Begueret, J. (1997) The protein product of the het-s heterokaryon incompatibility gene of the fungus *Podospora anserina* behaves as a prion analog, *Proc. Natl. Acad. Sci. U.S.A. 94*, 9773−9778.
4. Cohen, F. E., Pan, K. M., Huang, Z., Baldwin, M., Fletterick, R. J., and Prusiner, S. B. (1994) Structural clues to prion replication, *Science 264*, 530−531.
5. Sipe, J. D., and Cohen, A. S. (2000) History of amyloid fibril, *J. Struct. Biol. 130*, 88−98.
6. Koo, E. H., Lansbury, P. T., Jr., and Kelly, J. W. (1999) Amyloid diseases: abnormal protein aggregation in neurodegeneration, *Proc. Natl. Acad. Sci. U.S.A. 96*, 9989−9990.
7. Taylor, J. P., Hardy, J., and Fischbeck (2002) Toxic proteins in neurodegenerative disease, *Science 296*, 1991−1995.
8. Lacroute, F. (1971) Non-Mendelian mutation allowing ureidosuccinic acid uptake in yeast, *J. Bacteriol. 106*, 519−522.
9. Magasanik, B. (1992) in *The Molecular and Cellular Biology of the Yeast Saccharomyces cerevisiae* (Jones, E. W., Pringle, J. R., and Broach, J. R., Eds.) Vol. 2, pp 283−317, Cold Spring Harbor Laboratory Press, Plainview, NY.
10. Masison, D. C., and Wickner, R. B. (1995) Prion-inducing region of yeast Ure2p and protease resistance of Ure2p in prion-containing cells, *Science 270*, 93−95.
11. Coschigano, P. W., and Magasanik, B. (1991) The URE2 gene product of *Saccharomyces cerevisiae* plays an important role in the cellular response to the nitrogen source and has homology to glutathione S-transferases, *Mol. Cell. Biol. 11*, 822−832.
12. Thual, C., Komar, A. A., Bousset, L., Fernandez-Bellot, E., Cullin, C., and Melki, R. (1999) Structural Characterization of *Saccharomyces cerevisiae* Prion-like Protein Ure2, *J. Biol. Chem. 274*, 13666−13674.
13. Bousset, L., Belrhali, H., Janin, J., Melki, R., and Morera, S. (2001) Structure of the Globular Region of the Prion Protein Ure2 from the Yeast *Saccharomyces cerevisiae*, *Structure 9*, 39−46.
14. Umland, T., Taylor, K. L., Rhee, S., Wickner, R. B., and Davies, D. R. (2001) The crystal structure of the nitrogen regulation fragment of the yeast prion protein Ure2p, *Proc. Natl. Acad. Sci. U.S.A. 98*, 1459−1464.
15. Masison, D. C., Maddelein, M. L., and Wickner, R. B. (1997) The prion model for [URE3] of yeast: spontaneous generation and requirements for propagation, *Proc. Natl. Acad. Sci. U.S.A. 94*, 12503−12508.

16. Bousset, L., Thomson, N. H., Radford, S. E., and Melki, R. (2002) The yeast prion Ure2p retains its native alpha-helical conformation upon assembly into protein fibrils in vitro, *EMBO J. 21*, 2903−2911.
17. Taylor, K. L., Cheng, N., Williams, R. W., Steven, A. C., and Wickner, R. B. (1999) Prion domain initiation of amyloid formation in vitro from native Ure2p, *Science 283*, 1339−1343.
18. Holmes, K. C., Popp, D., Gebhard, W., and Kabsch, W. (1990) Atomic model of the actin filament, *Nature 347*, 44−49.
19. Nogales, E., Whittaker, M., Milligan, R. A., and Downing, K. H. (1999) High-resolution model of the microtubule, *Cell 96*, 79−88.
20. Huntington, J. A., Pannu, N. S., Hazes, B., Read, R. J., Lomas, D. A., and Carrell, R. W. (1999) A 2.6 Å structure of a serpin polymer and implications for conformational disease, *J. Mol. Biol. 293*, 449−455.
21. Liu, Y., Gotte, G., Libonati, M., and Eisenberg, D. (2001) A domain-swapped RNase A dimer with implications for amyloid formation, *Nat. Struct. Biol. 8*, 211−214.
22. Bousset, L., Briki, F., Doucet, J., and Melki, R. (2003) The native-like conformation of Ure2p in fibrils assembled under physiologically relevant conditions switches to an amyloid-like conformation upon heat-treatment of the fibrils, *J. Struct. Biol. 141*, 132−142.
23. Speransky, V. V., Taylor, K. L., Edskes, H. K., Wickner, R. B., and Steven, A. C. (2001) Prion filament networks in [URE3] cells of *Saccharomyces cerevisiae*, *J. Cell Biol. 153*, 1327−1336.
24. Baxa, U., Taylor, K. L., Wall, J. S., Simon, M. N., Cheng, N., Wickner, R. B., and Steven, A. C. (2003) Architecture of Ure2p prion filaments: The N-terminal domains form a central core fiber, *J. Biol. Chem. 278*, 43717−43727.
25. Thual, C., Bousset, L., Komar, A. A., Walter, S., Buchner, J., Cullin, C., and Melki, R. (2001) Stability, Folding, Dimerization, and Assembly Properties of the Yeast Prion Ure2p, *Biochemistry 40*, 1764−1773.
26. Spudich, J. A., and Watt, S. (1971) The regulation of rabbit skeletal muscle contraction. I. Biochemical studies of the interaction of the tropomyosin-troponin complex with actin and the proteolytic fragments of myosin, *J. Biol. Chem. 246*, 4866−4871.
27. Eisenberg, E., and Kielley, W. W. (1974) Troponin-tropomyosin complex. Column chromatographic separation and activity of the three, active troponin components with and without tropomyosin present, *J. Biol. Chem. 249*, 4742−4748.
28. Melki, R., Fievez, S., and Carlier, M. F. (1996) Continuous monitoring of Pi release following nucleotide hydrolysis in actin or tubulin assembly using 2-amino-6-mercapto-7-methylpurine ribonucleoside and purine-nucleoside phosphorylase as an enzyme-linked assay, *Biochemistry 35*, 12038−12045.
29. MacLean-Fletcher, S., and Pollard, T. D. (1980) Identification of a factor in conventional muscle actin preparations which inhibits actin filament self-association, *Biochem. Biophys. Res. Commun. 96*, 18−27.
30. Shelanski, M. L., Gaskin, F., and Cantor, C. R. (1973) Microtubule assembly in the absence of added nucleotides, *Proc. Natl. Acad. Sci. U.S.A. 70*, 765−768.
31. Weingarten, M. D., Lockwood, A. H., Hwo, S. Y., and Kirschner, M. W. (1975) A protein factor essential for microtubule assembly, *Proc. Natl. Acad. Sci. U.S.A. 72*, 1858−1862.
32. McParland, V. J., Kad, N. M., Kalverda, A. P., Brown, A., Kirwin-Jones, P., Hunter, M. G., Sunde, M., and Radford, S. E. (2000) Partially unfolded states of b2-microglobulin and amyloid formation in vitro, *Biochemistry 39*, 8735−8746.
33. Laemmli, U. K. (1970) Cleavage of structural proteins during the assembly of the head of bacteriophage T4, *Nature 227*, 680−685.
34. Morrissey, J. H. (1981) Silver stain for proteins in polyacrylamide gels: A modified procedure with enhanced uniform sensitivity, *Anal. Biochem. 117*, 307−310.
35. Khurana, R., Uversky, V. N., Nielsen, L., and Fink, A. L. (2001) Is Congo red an amyloid-specific dye?, *J. Biol. Chem. 276*, 22715−22721.
36. Elghetany, M. T., Saleem, A., and Barr, K. (1989) The congo red stain revisited, *Ann. Clin. Lab. Sci. 19*, 190−195.
37. Zurdo, J., Guijarro, J. I., and Dobson, C. M. (2001) Preparation and characterization of purified amyloid fibrils, *J. Am. Chem. Soc. 123*, 8141−8142.
38. Sunde, M., Serpell, L. C., Bartlam, M., Fraser, P. E., Pepys, M. B., and Blake, C. C. (1997) Common core structure of amyloid fibrils by synchrotron X-ray diffraction, *J. Mol. Biol. 273*, 729−739.
39. Perrett, S., Freeman, S. J., Butler, P. J., and Fersht, A. R. (1999) Equilibrium folding properties of the yeast prion protein determinant Ure2, *J. Mol. Biol. 290*, 331−345.
40. Baxa, U., Speransky, V., Steven, A. C., and Wickner, R. B. (2002) Mechanism of inactivation on prion conversion of the *Saccharomyces cerevisiae* Ure2 protein, *Proc. Natl. Acad. Sci. U.S.A. 99*, 5253−5260.
41. Amos, L. A. (1985) Structure of muscle filaments studied by electron microscopy, *Annu. Rev. Biophys. Biophys. Chem. 14*, 291−313.
42. Van Loock, M. S., Yu, X., Yang, S., Lai, A. L., Low, C., Campbell, M. J., and Egelman, E. H. (2003) ATP-mediated conformational changes in the RecA filament, *Structure (Cambridge) 11*, 187−196.
43. Lowe, J., and Amos, L. A. (1999) Tubulin-like protofilaments in Ca^{2+}-induced FtsZ sheets, *EMBO J. 18*, 2364−2371.
44. Gregoire, C., Marco, S., Thimonier, J., Duplan, L., Laurine, E., Chauvin, J. P., Michel, B., Peyrot, V., and Verdier, J. M. (2001) Three-dimensional structure of the lithostathine protofibril, a protein involved in Alzheimer's disease, *EMBO J. 20*, 3313−3321.
45. Lomas, D. A., and Carrell, R. W. (2002) Serpinopathies and the conformational dementias, *Nat. Rev. Genet. 3*, 759−768.
46. Westermark, P., Benson, M. D., Buxbaum, J. N., Cohen, A. S., Frangione, B., Ikeda, S., Masters, C. L., Merlini, G., Saraiva, M. J., and Sipe, J. D. (2002) Amyloid fibril protein nomenclature—2002, *Amyloid 9*, 197−200.
47. Fernandez-Bellot, E., Guillemet, E., and Cullin, C. (2000) The yeast prion [URE3] can be greatly induced by a functional mutated URE2 allele, *EMBO J. 19*, 3215−3222.
48. Gouet, P., Courcelle, E., Stuart, D. I., and Metoz, F. (1999) ESPript: multiple sequence alignments in postcript, *Bioinformatics 15*, 305−308.

BI049828E